

Cleaning Up Noise Power Measurements Using Control Charts

*Paul J. Kane and Robert E. Cookingham
Eastman Kodak Company, Rochester, NY USA*

Abstract

The Wiener or noise power spectrum (NPS) is a well-known tool in the assessment of image noise. Normally the spectrum is computed from digital data representing an image at some stage of processing, scans of film, or scans of a hardcopy output medium. In preparing the NPS estimation, the data frequently contain defects, which affect the resulting spectral estimate. These defects include density gradients (non-stationary mean), scratches, dust, coating defects (outliers), signal processing induced artifacts, or images of any of the above defects on a printed image. Drift of the mean and outliers causes a bias in the spectral estimate at low spatial frequencies.

In this paper, we describe a method employing the classical statistical process control tool of control charts as a test to indicate that all non-random signals have been removed from the test data set. To demonstrate the method, we use the periodogram method of spectral estimation, in which the scanned data is grouped into short segments. The effect of the mean drift can be suppressed by subtracting a linear least squares fit from each segment. Control chart methodology is applied in the data processing, assuming the digital data are normally distributed. The control chart is used to identify data segments containing outliers. These segments can then be excluded from the spectral estimate, resulting in improved noise power spectrum and RMS granularity measurements.

Introduction

Methods for the estimation of NPS, and the subsequent estimation of RMS granularity, are well-known in the literature.¹ We use the periodogram method of spectral estimation, based on short data sequences. This facilitates trend removal and outlier rejection. We begin with a microdensitometer trace of a uniformly exposed transparency or reflection print, taken with a long, narrow slit. Equivalently, a 1-D slit scan can be synthesized from 2-D scanner data. For isotropic random noise, analysis of the 1-D slit scan yields a slice through the rotationally symmetric 2-D NPS surface. The NPS estimator is:

$$\hat{NPS}(v_k) = \frac{L\Delta x}{MN} \sum_m \left| \sum_n \Delta D_m(n\Delta x) e^{-i2\pi kn/N} \right|^2 \quad (1)$$

where $\Delta D_m(x)$ is the optical density fluctuation at point x in the m^{th} segment (out of M total segments), v_k is the k^{th} spatial frequency, Δx is the sample spacing, L is the length of the scanning slit, and N is the number of points per segment. The discrete Fourier Transform indicated in Eq. (1) yields an NPS estimate at a series of spatial frequencies spaced at $\Delta v = v_{k+1} - v_k = 1/(N\Delta x)$.

The RMS granularity associated with a circular aperture of radius r can be computed from this 1-D NPS estimate by the following equation:

$$\sigma_D^2 = \frac{2\Delta v}{\pi r^2} \sum_k \hat{NPS}(v_k) \frac{J_1^2(2\pi r v_k)}{v_k} \quad (2)$$

where $v_k > 0$ and J_1 is the first-order Bessel function of the first kind.

Generally we hypothesize that the microdensity data from a flat field image represent samples from a 2-D Gaussian, ergodic random process, which is the source of the perceived graininess seen in the image. Under these conditions, the estimators given in Eq. (1) and Eq. (2) converge to the population values in the limit of large data sets. Other, non-random sources of density variation in the scan data, such as density gradients (trends), or the large localized density excursions produced by coating and exposure defects (outliers), lead to low-frequency bias in the estimate.² Although these defects may also be visible and objectionable in the image, we do not wish to include them in the NPS and RMS granularity estimates, which are taken to be objective correlates of graininess, rather than large scale non-uniformities. The main subject of this paper is a technique for outlier identification and removal.

Trend and Outlier Removal

The need to remove non-stationary behavior and other non-random variations prior to spectral estimation has been recognized in the literature.³ Preprocessing of the data is not without pitfalls, however, and must be done carefully in order to avoid introducing other unwanted biases into the spectral estimate as an unintended side effect. The signal processing literature contains some very sophisticated techniques for the robust estimation of power spectra.^{4,5} Our emphasis here is on techniques that, while

not as rigorous or powerful as some others that have been proposed, have the advantages of simplicity and efficiency, while maintaining a strong statistical foundation.

Trend removal is the first step in preprocessing, and is often accomplished by fitting a linear or polynomial equation to the microdensity trace. A more complex functional form is justified in situations where a priori knowledge of the non-stationary components is available. Note that the removal of density drift in the input data corrects for non-stationary components in the mean value of the process, but not the variance. This is important if the noise exhibits a strong signal dependence. In our experience, transparencies and prints of photographic quality contain density gradients that can be modeled as piecewise linear drifts in the mean, over the segment lengths typically chosen for NPS analysis. Hence, our strategy is to perform a linear least squares regression on each segment of data, and to then subtract the fit from each segment. One side effect of any subtractive approach is the loss of the zero frequency NPS estimate.⁶ Fortunately, this loss is not catastrophic, as most NPS curves are monotonic (allowing for robust extrapolation), and the zero frequency is naturally excluded from the RMS granularity estimate of Eq. (2).

The second step in preprocessing is outlier removal. If the data of interest are presumed to follow a normal or Gaussian distribution, a test for normality is indicated. The Gaussian assumption is a good one, particularly for natural sources such as photographic granularity or electronic noise. In digital systems, components of limited bit depth may introduce textures that are demonstrably non-Gaussian, through a rendering algorithm such as error diffusion or periodic dither. In these cases, a normality test may not be appropriate.

Many tests for normality have been described in the literature.³ Since our NPS estimation technique is based on segmentation of the data, we favored a segment-based approach. This class of approach, based on segmentation or grouping of the data, has been quite successful in the direct estimation of RMS granularity.⁷ The strategy is to identify and remove outlying segments, rather than individual points. With this approach in mind, we turned to the methodology of control charts.

Control Chart Methods

Although classical control chart methods were originally developed to monitor and improve manufacturing processes,⁸ these techniques provide a tool for determining and analyzing the stability of research instruments and the data collected using them. In the technique described in this work, we use a control chart to examine the data collected with a microdensitometer and eliminate scan segments that are not the random noise components expected from a microdensitometer trace of a uniform neutral material. We treat the scan as a set of independent and randomly distributed density measurements and any data segments that exceed the control chart limits arise from a spurious causal

mechanism, which disqualifies them from inclusion in the NPS calculation.

To apply the control chart method, a series of measurements within a block of microdensitometer measurements are considered to be a rational subgroup. A rational subgroup is defined as a set of observations within which the variations may be considered on engineering grounds to be due to non-assignable or random causes. Control limits, (upper control limit UCL and lower control limit LCL) are derived according to the standard formulas⁹ for the central tendency given in Eqs. (3) and (4). In a control chart for the sample means (the X-bar chart), the centerline is the mean of the subgroup means (X double-bar), and the number of data points in each subgroup is denoted as N .

$$UCL_{\bar{X}} = \bar{\bar{X}} + 3 \cdot \frac{\bar{s}}{\sqrt{N}} \quad (3)$$

$$LCL_{\bar{X}} = \bar{\bar{X}} - 3 \cdot \frac{\bar{s}}{\sqrt{N}} \quad (4)$$

Good practice requires that two control charts be maintained to monitor trends in both the mean and variation for a process under evaluation. For the control chart monitoring the variation (the s chart), \bar{s} is the mean standard deviation of all of the subgroups (or blocks), UCL is the upper variation control limit, and LCL is the lower variation control limit. The formulas for calculating the variation limits are given in Eqs. (5) and (6).

$$UCL_s = \bar{s} + 3 \cdot \frac{\bar{s}}{\sqrt{2(N-1)}} \quad (5)$$

$$LCL_s = \bar{s} - 3 \cdot \frac{\bar{s}}{\sqrt{2(N-1)}} \quad (6)$$

Once the control chart limits have been established and data segments that lie outside the 3σ UCL and LCL limits have been discarded, a number of other criteria are applied to the data segments. These criteria are designed to detect trends or unnatural patterns in the data, which are associated with a non-random or systematic pattern. The criteria are based on the probability of significant patterns of data points occurring in the data sequence. The area between the upper and lower control limits is divided into six zones spaced in one standard deviations (σ) increments. Using these zones the criteria are:

Tests for instability

- 1 point $> 3\sigma$
- 2 out of 3 points $> 2\sigma$
- 4 out of 5 point $> 1\sigma$

- 8 points in a row above or below the centerline

Test for Stratification

- 15 or more points $< |\sigma|$

Test for a multi-modal behavior

- 8 or more points $> |\sigma|$

Tests for a systematic variation

- A long series of points with a high – low or a periodic pattern.

In our NPS estimation procedure, a control chart is initially constructed using the segment means, to aid in the detection of trends. In most cases, the need for some level of trend removal is indicated, and the piecewise linear regression technique is applied. At that point, the mean has been essentially removed from the data, and further analysis is based on the variation control chart (segment standard deviations). The tests indicated above are applied to the segment standard deviations, and outlying segments are identified. The tests are applied in the order given above, with the following modifications. The upper and lower control limits are established via Eqs. (5) and (6); if Eq. (6) yields a result less than zero, then the lower control limit is set to zero (since by definition the standard deviation is a positive number). We then begin with the first of the instability tests, which searches for segment standard deviations exceeding the 3σ limits. These are discarded first, and then the upper and lower control limits are recomputed. This was found to be necessary in practice to guard against extreme outliers, which bias the calculated control limits themselves, preventing meaningful application of the remaining tests.

In the tests that apply to “runs” of segments, the exclusion of segments proceeds as demonstrated in the following example. In the second instability test, the control chart is examined in the “2 to 3 σ ” zone. Starting from the beginning, the first three segments ($j = 1,2,3$) are examined. If two out of the three segment standard deviations are simultaneously greater than the upper control limit, or simultaneously less than the lower control limit, then the second segment that is outside the limit is marked for exclusion. The other two segments in the group of three are retained. The next group of three to be examined depends on the last “good” segment in the previous group. For example, if all three segments had passed the test, the next group of three to be examined would be segments $j = 2,3,4$. If the second segment had failed, then the next group examined would be $j = 3,4,5$. If the third segment had failed, the next group examined would be $j = 4,5,6$. The process continues until all segments have been examined.

After all the tests have been applied to all the segments, the segments marked for exclusion are removed, and the control limits are recalculated. The process then resumes from the beginning, until the number of iterations exceeds some preset limit, or preferably until all segments pass all of the tests (or all segments have failed). Thus, the algorithm has a built-in stopping criterion with a sound

statistical basis, which arbitrary empirical methods lack. We have demonstrated that the algorithm does not remove segments from “clean” computer generated data. Thus, we are assured that the algorithm decreases the risk of a positive bias error in the NPS for data sequences corrupted by outliers, but does not pose the risk of a negative bias error in the absence of outliers.

NPS Examples

Figure 1 shows two variation control charts, generated from a microdensitometer slit scan of a flat field in a reflection print. The standard deviation of each segment has been plotted as a function of the segment number. We began with 256 segments, each containing 128 points. The top control chart shows the segment standard deviations, after the piecewise linear trend removal has been applied. The presence of segments outside of the 3σ zone is apparent; careful inspection of the chart reveals the presence of other unnatural patterns. The bottom control chart shows the status of the segments, after the outlier rejection algorithm has been applied iteratively until no further segments are excluded. Inspection of this chart demonstrates that the unnatural patterns have been removed. Note that the number of segments has been reduced to 168 out of the original 256. The bias in the NPS estimate, because of outliers, is thus eliminated at the expense of a small loss of statistical precision in the overall estimate. The standard error of the estimate is given by:¹

$$SE = \frac{1}{\sqrt{M}} \quad (7)$$

where SE is the standard error of the NPS estimate at each frequency, and M is the total number of segments.

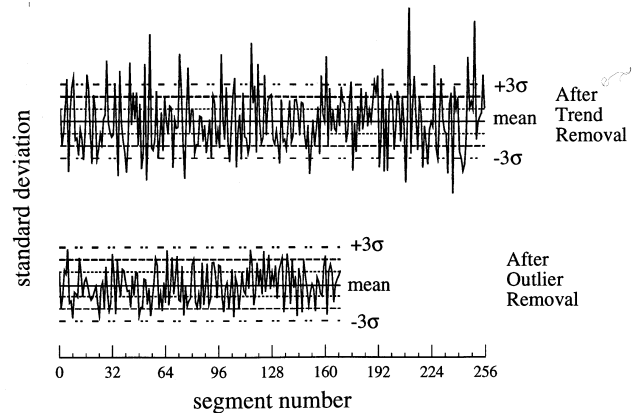


Figure 1. Control charts before and after outlier removal.

Figure 2 shows the raw NPS estimate, using all 256 segments (solid line). The estimate shows evidence of nonstationarity in the mean of the data, as demonstrated by the sudden increase in the NPS at zero spatial frequency. The presence of outliers is not always evident in the NPS curve. The dotted curve in Fig. 2 shows the NPS estimate after linear trend removal. The zero frequency NPS estimate has been lost; there has been some reduction in

the estimate between 0.25 and 1.25 cycles/mm. The long-dashed curve in Fig. 2 shows the result of subsequent application of the control chart algorithm. A further reduction in the NPS over the band 0.25 to 1.25 cycles/mm is observed. Finally, the short-dashed line in Fig. 2 demonstrates the behavior of the NPS estimate for a data set consisting of computer-generated random numbers. In this case, the process is stationary, the zero frequency NPS estimate is stable, and no outlier removal is required, as expected.

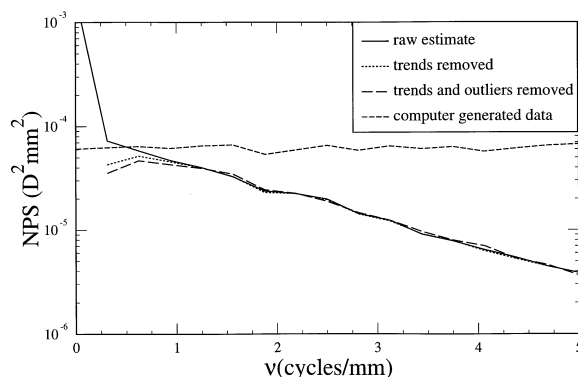


Figure 2. NPS estimates with and without preprocessing.

RMS Granularity Estimates

As Fig. 2 shows, the effect of the outlier identification and removal procedures on the NPS estimate may appear subtle. However, subtle changes in the NPS estimate may imply significant changes in predicted graininess, particularly if they occur at spatial frequencies that are visually important. Figure 3 shows the series of RMS granularity measurements for each step on the black and white grain ruler developed by Maier and Miller,¹⁰ obtained via NPS estimation and application of Eq. (2). The solid circles represent the estimated RMS granularity of each step, with no trend or outlier removal applied. The solid triangles represent the adjusted estimates, using trend and outlier removal. The log of 1000 times the RMS granularity is plotted on the y-axis, with tic marks at 0.05 log units, or about twice the value of a just noticeable difference (JND) in granularity for a uniform field (1 JND in graininess = a 6% change in RMS granularity¹¹). Preprocessing of the data before NPS estimation reduces all of the RMS granularity estimates, and has a major impact on the estimates at the lowest steps on the ruler. In particular, the raw estimates would predict that step 2 might exhibit slightly higher graininess than step 3, which is not consistent with direct observations of the graininess. Furthermore, the estimate of the RMS granularity of step 1 is reduced from about 4.5 (RMS times 1000) to about 2.5, a difference which is about 10 times the JND, and again more consistent with direct observation of the graininess. In general, we have found that application of trend removal

and the control chart outlier removal algorithm has lowered our detectability of granularity in hardcopy photographic prints from around 5 (RMS times 1000) to 2, a significant increase in sensitivity.

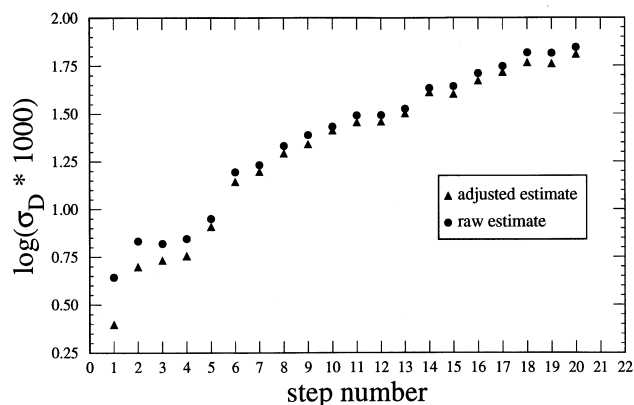


Figure 3. RMS granularity of black and white grain ruler steps.

Conclusion

The control chart methodology enables significant improvements in noise power spectrum and RMS granularity measurement capability. Using this method, we have been able to lower the threshold of detectability for hardcopy photographic print media granularity measurements made with a microdensitometer to $\sigma_d < 2$, approximately a 60% reduction from the previous value of $\sigma_d = 5$ (RMS times 1000).

References

1. J. C. Dainty and R. Shaw, *Image Science*, Academic Press, New York, 1974, pg. 215.
2. M. Wolf and W. Angerstein, *Phys. Med. Biol.* **32**, 557 (1987).
3. J. S. Bendat and A. G. Piersol, *Random Data: Analysis and Measurement Procedures*, Wiley, New York, 1986, Ch. 11.
4. R. D. Martin and D. J. Thomson, *Proc. IEEE* **70**, 1097 (1982).
5. A. D. Chave, D. J. Thomson and M. E. Ander, *J. Geophys. Res.* **92**, 633 (1987).
6. P. D. Burns and B. M. Levine, *J. Appl. Photogr. Eng.* **9**, 78 (1983).
7. E. Buhr, S. Richter and D. Hoeschen, *PTB-Mitteilungen* **101**, 183 (1991).
8. W. A. Shewhart, *Economic Control of Manufactured Product*, Van Nostrand, New York, 1931.
9. ASTM Manual on Presentation of Data and Control Chart Analysis, Prepared by Committee E-11 on Statistical Methods, American Society for Testing and Materials, STP 15D, American Society for Testing and Materials, Philadelphia, 1976.
10. T. O. Maier and D. L. Miller, *Proc. SPSE's 43rd Annual Conference*, 1990, p. 207.
11. D. Zwick and D. L. Brothers, *SMPTE J.* **86**, 427 (1977).